LA-UR-83-2138

Conf-830719--21

Los Alamos National Laboratory is operated by the University of California for the United States Department of Energy under contract W-7405-ENG-36

TITLE THRE.:-DIMENSIONAL COMPUTER MODELING OF A SHOCK-RECOVERY EXPERIMENT

LA-UR--83-2138

DE83 015915

AUTHOR(S) R. L. Rab. . Vorthman, and J. K. Dienes

SUBMITTED TO Third American Physical Society Topical Conference
Held in Santa Fe, New Mexico
July 18-21, 1983

MASTER

Los Alamos

Los Alamos National Laboratory
Los Alamos, New Mexico 87545

FORM NO. 836 R4
ST. NO. 2629 5/81

DISTRIBUTION OF THIS DOCUMENT IS UNLIMITED

THREE-DIMENSIONAL COMPUTER MODELING OF A SHOCK-RECOVERY EXPERIMENT

R. L. Rabie, J. E. Vorthman, and J. K. Dienes

Los Alamos National Laboratory
Los Alamos, New Mexico

An ideal shock recovery experiment would be to subject a sample material to a single, well-defined shock followed by a controlled, benign release of the stresses and velocities generated. The process should be such that any change found in the sample after recovery could be attributed to the shock process alone. In any real experiment with finite-sized samples, rarefaction waves are generated at the edges of the sample. In general these rarefaction waves can have a large effect on the sample, which is impossible to separate from the effects of the shock alone. It has been suggested that samples of certain shapes will have a small region in their interiors, which is substantially free from the effects of edge rarefactions. We will present the results of three-dimensional computer calculations done to test this hypothesis.

1. INTRODUCTION

Vorthman and Duvall employed a star-shaped sample as a means of mitigating lateral release wave effects at the sample center in their work on lithium flouride (LiF).[1] The particular experimental arrangement they used was a modification of a technique originally proposed and used by Kumar and Clifton.[2] Both of these shock recovery ideas rely on three-dimensional attenuation effects. Other techniques, known to be fairly successful, involve the use of guard rings in two-dimensional shock recovery experiments.[3-4] Numerical calculations of impacts involving the guard ring configuration have been done by Stevens and Jones.[5] In this paper, we present preliminary numerical calculations of a prototype three-dimensional impact problem in which a star-shaped sample, thin with respect to its average diameter, is studied. The shape selected is that of Vorthman and Duvall, shown in Figure 1, and the impact of the star is onto a rigid boundary. The material is assumed to be annealed 2024 Aluminum and the impact velocity is 0.17 mm/μs. The constitutive relation is elastic-perfectly plastic, and we have taken a yield strength in simple tension of 1 kbar.[6] For comparison, we have also run an impact problem using a thin square plate as a sample. The cases of the thin square plate and the thin star show, quite graphically, the improved results for the star geometry.

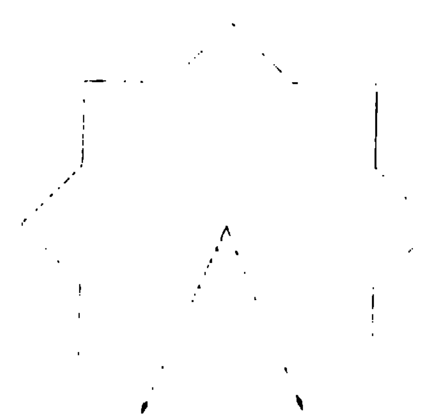

Figure 1 : Sample shape and region calculated. Y is normal to the page.

2. THEORY

We use the simplest elastic-plastic constitutive assumption, elastic perfectly plastic. The system behaves as linear elastic material until the scalar product of the stress deviator tensor exceeds $2/3\ Y_0^2$, where Y_0 is the yield stress in simple tension. When yield occurs, the stress deviators are returned normally to the yield surface, which amounts to multiplying each of the deviator components by a constant, thereby reducing the scalar product of the stress deviators to the value $2/3\ Y_0^2$. The total strain is known and the amount of elastic deviator strain supported by the adjusted stress deviators is known. These facts, together with the assumption that the trace of the velocity gradient tensor is not altered by plastic strain allows partitioning of the total strain into the elastic and plastic parts. Work hardening is often accounted for by making the yield strength a function of the plastic work and stress relaxation is accounted for by assuming the factor used to adjust the stress deviators back to the yield surface is a function of time. Neither stress relaxation nor work hardening are used in these calculations. This results in more plastic flow than would occur in the real material rendering these calcuations conservative.

The material hydrostat is assumed to be given by a Grüneisen equation-of-state. This equation-of-state is calibrated to a linear shock-particle velocity relation for 2024 Aluminum. Equation-of-state and constitutive parameters are shown in Table I.

TABLE I
Equation-of-State & Constitutive Parameters for 2024 Aluminum

ρ_0 (density)	2.785 g/cc
λ (Lame Constant)	61.000 GPa
μ (Lame Constant)	25.000 GPa
Y_0 (Yield in Simple Tension)	.100 GPa
C (Constant in $C + SU_p$)	5.328 mm/μs
S (Constant in $C + SU_p$)	1.338
Γ (Grüneisen Ratio)	2.0

3. CALCULATIONS

3.1 General

The results of the calculations are presented as a series of views of the samples and their interiors. We have plotted only mean pressure. The perspective plots may be understood by recourse to the cell zoning convention of the Lagrangian code. The index i denotes points on the "α" coordinate axis, j points on the "β" coordinate axis, and the k points on the "γ" coordinate axis. Thus, for a computational mesh having nx zones of $\Delta\alpha$ size in the "α" direction, ny zones of $\Delta\beta$ size in the "β" direction, and nz zones of $\Delta\gamma$ size in the "γ" direction, a plot of pressure on the k = 5 surface takes a surface at "γ" = 5 $\Delta\gamma$ and plots the pressure contours that exist on that surface at the selected times. We use the notation "α," "β," and "γ" because the code we use (an extensive modification of SALE 3D)[7] allows arbitrary boundary shapes resulting in "α," "β," and "γ" material coordinates that are generally not linear or orthogonal. For example, in the star calculations presented in this paper the sample boundaries in the "α-β" plane are initially linear but they are not orthogonal. One of the consequences of this is that a surface of constant cell index is generally not planar. Finally, we emphasize that the runs we are presenting and the interpretations we are making are preliminary. The flows are extremely complex. The star calculation used a computing mesh of 15,028 cells ($34(\alpha) \times 34(\beta) \times 13(\gamma)$). This calculation required approximately 1.5 hours of Cray 1 CPU time to obtain 1.0 μs physical time.

3.2 The Square Plate

As a preliminary to the calculation of the star, we calculated a thin square plate impact problem. The plate dimensions were 11.2 mm square by 1.5-mm thick. The plate and the actual region calculated are shown in Figure 2.

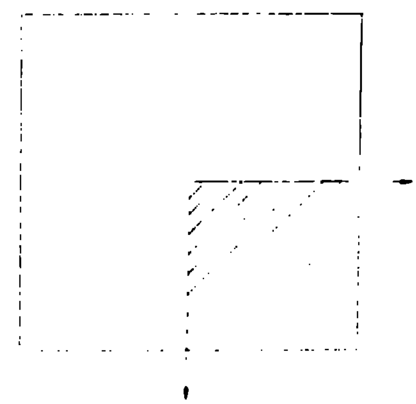

Figure 2 : Sample shape and region calculated

Because of symmetry, we calculated only one quarter of the plate on a mesh of $20(\alpha) \times 20(\beta) \times 13(\gamma)$ cells. Figures 3-5 are views of the plate from above with pressure contours plotted on the plate midplane (~0.75 mm from the plate bottom).

The plots are at times of 0.5, 1.0, and 2.2 μs after impact, respectively. Three features of the flow are important. First, plastic flow occurs in the corners where the converging rarefactions from the sample edges result in large tensions (10 kbars at t = 0.5 μs in Figure 3). Second, the edge rarefactions reach the sample center and reflect there, leaving a region of tension (-4 kbars at t = 2.2 μs in Figure 5). Views of this region from the side, Figure 6, show a two-dimensional flow field at the sample center.

Surprisingly, not a great deal of yield has occurred at 2.2 μs at the sample center. We have not run this case beyond 2.2 μs. Third, the plate is allowed to rebound from the rigid impact surface (γ = 0.0). The lateral flow at the plate edges causes the edges to remain nearer the boundary than the plate center during the rebound. Thus, the plate acquires a curvature (middle high - edges low) as it flies free of the rigid boundary. We will return to this fact in the case of the star. Finally, it is worth noting that the edge rarefactions, as they approach the sample center, are having to travel through a series of waves. These waves are alternate releases and compressions that travel through the sample thickness. They are residuals of the initial shock and release that loaded and unloaded the sample. We have, as yet, been unable to sort out all the details of this aspect of the calculations.

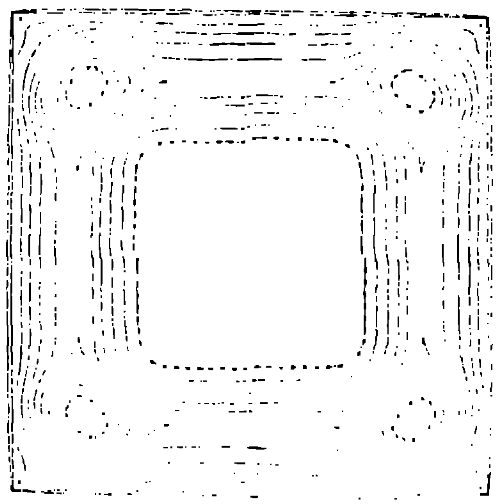

Figure 3 : The square plate midplane (~0.75 mm) at time 0.5 μs. Pressure contours lie between H = 0.065 GPa and L = 1.0 GPa .

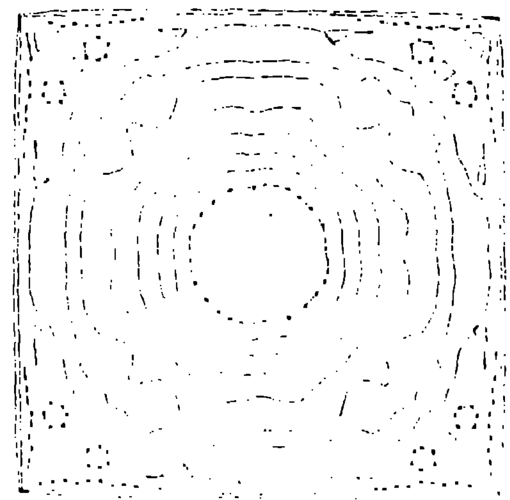

Figure 5 : The square plate midplane (~0.75 mm) at time 2.2 μs. Pressure contours lie between H = 0.003 GPa and L = 0.38 GPa.

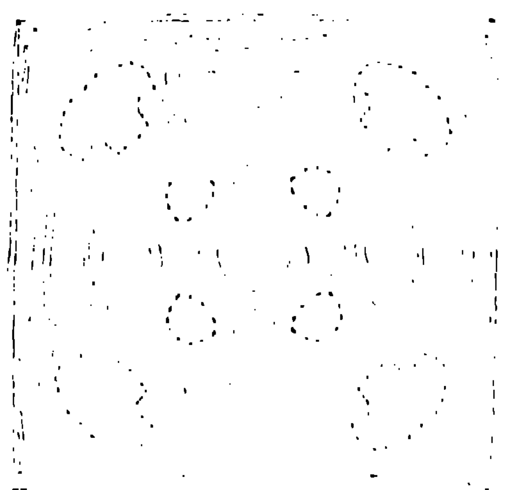

Figure 4 : The square plate midplane (~0.75 mm) at time 1.0 μs. Pressure contours lie between H = 0.057 GPa and L = 0.35 GPa.

Figure 6 : The square plate in cross section at time 2.2 μs. The plane is $\theta = 0$. Pressure contours lie between H = 0.046 GPa and L = 0.415 GPa.

3.3 The Star Plate

The general idea behind going to a star-shaped impact plate is to have the edge rarefactions directed away from the sample center so that they might have the opportunity to "get lost." Preliminary analysis of a star calculation (34(r) × 34(θ) × 13(z)) indicates that something like this "getting lost" does happen. The calculation has been run to 3 μs, 1.5 times the time required for the edge rarefactions to reach the sample center. We can find no evidence that rarefactions have reached the sample center at that time. Figures 7 and 8 show the star midplane (0.75 mm from the star bottom) at 0.5 and 1.0 μs after impact.

In Figure 7, the pressure ranges from 0.8 to 1.2 kbars and edge rarefactions have traveled to 3.5 mm. In Figure 8, the leading edge of the rarefaction is beginning to dissipate because of the divergence introduced at the

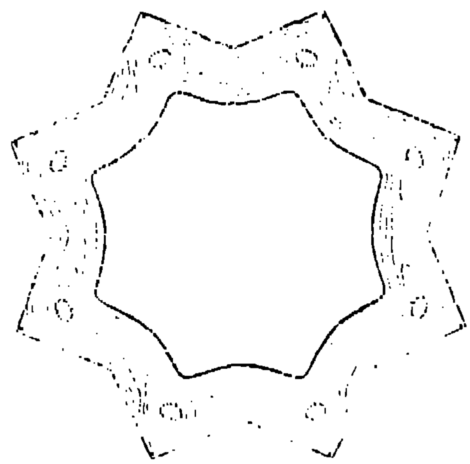

Figure 7 : The star plate midplane (~0.75 mm) at time 0.5 μs. Pressure contours lie between H = 0.123 GPa and L = 0.983 GPa.

Figure 8 : The star plate midplane (~0.75 mm) at time 1.0 μs. Pressure contours lie between H = 0.064 GPa and L = 0.461 GPa.

stars inside corners. Note also the onset of high pressure regions at the inside corners because of the convergent flow occurring there. The high pressure region beginning to grow at the star tips is not clearly understood. We believe it may be a consequence of a converging flow resulting from an elastic contraction of the edges of the star tips. The star begins its rebound in the plots ~0.6 μs after impact. In concert with the square plate, the star tips rebound with a smaller velocity than the star centers. An edge view of the star, looking down a normal to a plane drawn from the star center to an inside corner, is provided by Figure 9.

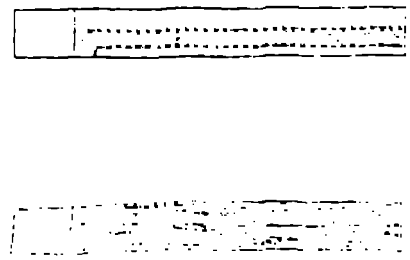

Figure 9 : The star plate crossection on α = 0 at times 0.1 μs and 1.9 μs. Pressure contours, respectively, are H = 2.28 GPa and L = 0.253 GPa; H = 0.197 GPa and L = 0.098 GPa.

These views are at t = 0.1 μs and 1.9 μs and show pressure contours on the plane just described. The view at 0.1 μs shows the initial shock. Vorthman notes that the stars recovered in his work on LiF all had the tips broken off. Figure 9 confirms that the star tips undergo a great deal of strain. It is evident that the flow in the bulk of the central section on the plane plotted here is one dimensional. We have not done an extensive series of these calculations, but this preliminary result is encouraging.

4. CONCLUSIONS

Preliminary calculations of a star-shaped sample undergoing shock loading indicate that this geometry may be an effective means of protecting the sample midsection from the effects of radial release. While the calculations are encouraging, more calculations with increased spatial resolution and longer runtime must be done to confirm this fact.

5. ACKNOWLEDGMENTS

The authors wish to thank H. Ruppel and J. Brackbill for helpful discussions.

References

1. J. F. Vorthman and G. E. Duvall, J. Appl. Phys. 53, 3607 (1982).
2. P. Kumar and R. J. Clifton, J. Appl. Phys. 48, 4850 (1977).
3. J. H. Smith, ASTM Special Technical Publication No. 336, 264-277 (1963).
4. W. F. Hartman, J. Appl. Phys. 35, 2090 (1964).
5. A. L. Stevens and O. E. Jones, J. Appl. Mech. 39, 359 (1972).
6. G. R. Fowles, J. Appl. Phys. 32, 1475 (1961).
7. A. A. Amsden and H. M. Ruppel, LA-8905, 1981.